Journal of Alloys and Compounds 867 (2021) 158880

Contents lists available at ScienceDirect

Journal of Alloys and Compounds

journal homepage: www.elsevier.com/locate/jalcom

Influence of Nb on Ti diffusion in γ-TiAl intermetallics studied by mechanical spectroscopy

J. Ibáñez-Pérez[a], M.L. Nó[b,*], M. Oehring[c], H. Clemens[d], J.M. San Juan[a]

[a] Dpt. Física Materia Condensada, Facultad de Ciencia y Tecnología, University of the Basque Country, UPV/EHU, Apdo. 644, 48080 Bilbao, Spain
[b] Dpt. Física Aplicada II, Facultad de Ciencia y Tecnología, University of the Basque Country, UPV/EHU, Apdo. 644, 48080 Bilbao, Spain
[c] Helmholtz-Zentrum Geesthacht, Institute for Materials Research, Max-Planck-Str. 1, 21502 Geesthacht, Germany
[d] Dpt. Materials Science, Montanuniversität Leoben, Roseggerstr. 12, 8700 Leoben, Austria

ARTICLE INFO

Article history:
Received 25 November 2020
Received in revised form 19 January 2021
Accepted 20 January 2021
Available online 2 February 2021

Keywords:
Intermetallics
Titanium aluminides
Internal friction
Diffusion
Point defects

ABSTRACT

The development of intermetallic titanium aluminides has been driven by the aeronautic and aerospace industries because of the excellent mechanical properties and low density of γ-TiAl based alloys. Up to now, several generations of γ-TiAl based alloys were developed with increasing complexity of the alloy systems. Nb is one of the most important alloying elements in γ-TiAl alloys and although it is considered as a slow diffuser, its influence has not been fully quantified yet. In this work we demonstrate, through mechanical spectroscopy measurements conducted on several γ-TiAl based alloys with different Nb content, that Nb impedes the diffusion of Ti atoms in the α_2-Ti_3Al phase. Internal friction measurements show a relaxation peak P(α_2), which is associated with short distance diffusion of Ti atoms in the α_2 phase, involving stress-induced rotation of dipoles Al-V_{Ti}-Al, whose activation energy is dependent on the Nb content. The increase of the activation energy is quantified as $\Delta E_a(Ti) = 0.037$ eV × at% Nb, being attributed to the next-neighbor interaction of Nb atoms with the local configuration of Ti-V_{Ti}. This mechanism also produces a further broadening of the relaxation peak, which is attributed to the near-next-neighbor interactions for high Nb contents. Finally, an atomic model for the mechanism responsible for this relaxation is proposed allowing to explain the observed experimental behavior.

1. Introduction

At the end of the last century, γ-TiAl based alloys were targeted as one of the most interesting materials for high-temperature applications. Its low density (≈ 4 g/cm^3), high elastic stiffness (double of Ni-superalloys), good oxidation resistance (up to 800 °C) as well as enhanced strength at high temperature made TiAl alloys very attractive to be used in aerospace and automotive engines [1–6]. Worldwide research activities have come a long way during the last two decades to overcome several obstacles, allowing move forward from fundamental aspects to real applications. The first generation of binary and ternary TiAl alloys [1,2] was followed by the development of a second generation of more advanced ternary and quaternary alloys: Ti–(45–48) Al–(1–3) Cr, Mn–(2–5) Nb, Ta, Mo at% [7,8]. Then, a third generation of Nb-rich Ti–45 Al–(5–10) Nb–(0–0.5) B, C at% alloys, termed TNB alloys, was developed to improve concurrently room temperature ductility and high temperature creep resistance [8–10]. In the last decade, a fourth generation of β-stabilized γ-TiAl alloys, with a well balanced amount of Nb and Mo, called TNM alloys, was designed to promote near conventional processing and allow to adjust long-term creep-resistant microstructures [11–13]. These international efforts succeed reaching commercial products in technological applications. Indeed, cast blades of the second generation of γ-TiAl based alloys, the so-called 48–2–2, are already introduced in the low-pressure turbine of the General Electric GEnx-1B engine [14], used in several aircrafts, as for instance the Boeing Dream Liner 787 [15]. The fourth generation of TNM alloys, is also being used in the low-pressure turbine of advanced aero-engines [16] and in racing applications, e.g. Formula 1 engines [6]. At present, the efforts are devoted to increase creep resistance through the introduction of controlled amounts of Si and C in the improved TNM$^+$ alloy family [17–20], as well as to extend the service temperature range by the addition of refractory metals such as W [21,22]. However, improving the material behavior at elevated temperatures requires a deep knowledge of the atomistic mechanisms controlling diffusion and dislocation climbing. The study of these processes can be approached by internal friction measurements through mechanical spectroscopy [23–26]. Indeed,

* Corresponding author.
E-mail address: maria.no@ehu.es (M.L. Nó).

https://doi.org/10.1016/j.jallcom.2021.158880
0925-8388/

since the pioneering works on the first generation γ-TiAl based alloys [27,28] as well as on second and third generation alloys [29–32], several internal friction studies were carried out on TNM alloys [33,34], on various Mo-rich γ-TiAl prototype alloys [35,36] and recently on TNM$^+$ alloys [37]. These studies allowed identifying several relaxation processes associated with short-distance atomic diffusion mechanisms in the different phases of TiAl alloys, namely γ-TiAl ($L1_0$, P4/mmm), α_2-Ti_3Al ($D0_{19}$, $P6_3/mmc$) and β_o-TiAl (B2, Pm-3 m) [8]. Although Nb is a slow diffuser in the α_2-Ti_3Al phase [38,39] and therefore is considered to impede the diffusion processes at high temperature [12], there is no a quantitative assessment of the influence of Nb on the diffusion of other atomic species and, in particular, on Ti self diffusion. Consequently, the objective of the present work is to elucidate such potential influence of Nb. With this idea in mind, it is worthy of mention that a relaxation process was associated with the short-distance Ti diffusion in α_2 phase [34,35,37], hence the dependence of this IF peak P(α_2) on the Nb content could offer a valuable information. Thus, in order to reach this goal, three γ-TiAl based alloys with different nominal Nb concentration were studied by mechanical spectroscopy and the obtained internal friction spectra were compared with the ones reported for other Nb leaner or even Nb-free γ-TiAl based alloys. Indeed, a quantitative analysis of the observed relaxation processes allows establishing the dependence of the activation energy for Ti diffusion in the α_2 phase on the prevailing Nb concentration.

2. Materials and methods

2.1. Samples and microstructural characterization

In order to study the influence of Nb on the diffusion processes, samples of three different alloys were measured by mechanical spectroscopy. Two samples were produced at the Helmholtz-Zentrum Geesthacht [8,40]. The first one with nominal composition Ti-45Al-8Nb-0.2C (at%) was extruded at 1200 °C, using a deformation ratio of 12:1, and subsequently was annealed 4 h at 1000 °C (it is named TNB8-Ex). The second alloy has a nominal composition of Ti-45Al-5Nb-0.2C-0.2B (at%) and was extruded at 1250 °C (ratio of 8:1), then forged parallel to the extrusion direction at 1150 °C and finally annealed 4 h at 1030 °C (it is named TNB-V5). Another sample, with a nominal composition Ti-45Al-5Nb-0.2C (at%), was made from thin sheets produced at Plansee SE, Austria, [5,6]. This sample was hot extruded (ratio of 7:1), then hot rolled and subsequently annealed 2 h at 1050 °C. Finally the specimen was heat treated at 1350 °C for 10 min, followed by gas quenching inside the furnace (it is named TNB5-PL). In the present study these three alloy variants are investigated and the obtained results are compared among each other and with a TNM4 alloy of nominal composition Ti-43Al-4Nb-1Mo-0.1B-0.02C (at%), which was produced at GfE, Germany, [11,41], whose internal friction spectra were previously measured [34], as well as with an another Nb-free alloy, i.e. Ti-46Al-1Mo-0.2Si (at%), termed TMS. This alloy was produced at the Max Planck Institute für Eisenforschung in Düsseldorf, Germany, [42] and was previously studied by mechanical spectroscopy as reported in [35]. The microstructures of the Nb containing alloys are shown in Fig. 1, evidencing that all of them are in the predominantly biphasic α_2+γ state, except the TNM4 alloy which additionally contains a small amount of β_o phase. Their compositions are summarized in Table 1. In addition, as the studied relaxation is taking place in the α_2 phase, a quantitative analysis of the Nb content in the α_2 phase was systematically conducted in all Nb containing alloys. The prevailing phases were identified by backscattered electron contrast in a field emission Focused Ion Beam, Helios Nanolab 650 from FEI, working at 10 keV, and quantitatively analyzed by energy dispersive X-ray spectroscopy (EDX), employing a Silicon Drift Detector from Oxford, with pure element standards and a beam current of 1 nA. This procedure was carried out in at least five different sites where several tens of analyses were performed to obtain a reliable average for each alloy. The average values of the Nb content existing in the α_2 phase are also included in Table 1.

2.2. Mechanical spectroscopy

Internal Friction (IF) and Dynamic Modulus (DM) variation measurements were carried out by mechanical spectroscopy in a high-temperature sub-resonant torsion pendulum described elsewhere [43,44]. The mechanical spectrometer works under high vacuum (< 10^{-5} mbar) in order to prevent oxidation of the specimen at high temperature. Samples in form of 50 × 5 × 1 mm^3 plates were cut by electro-discharge machining and then grinded and polished. A detailed description of the analysis procedures used in mechanical spectroscopy and its different working modes can be found in the literature, e.g. [23–26]. As described in these overviews, the IF is also denoted as Q^{-1}or $\tan\phi\,(\omega)$, with $\phi\,(\omega)$ being the lag angle between the strain and the stress during the application of the oscillating stress of angular frequency ω (this is what is measured in a sub-resonant pendulum), which should neither cause permanent deformation nor irreversible alteration of the microstructure. Therefore, we have used a maximum oscillation amplitude of $\varepsilon_0 = 2 \times 10^{-5}$ at room temperature to avoid any plastic deformation. Both IF and DM measurements were performed in forced oscillation mode for several frequencies ranging from 2.0 Hz down to 0.01 Hz, in a temperature range from 600 K to 1330 K, applying a heating rate of 1 K/min. The analysis of the relaxation peaks requires the subtraction of the high temperature background (HTB) and for this purpose the method of Schoeck et al. [45] was used, as described in the next section.

3. Experimental results

The occurrence of a relaxation IF peak P(α_2) was reported in the literature for several γ-TiAl based alloys, e.g. see [29–35,37], which was finally attributed to short distance diffusion of Ti atoms in the α_2 phase. It takes place by exchange of a Ti atom with a vacancy, V_{Ti}, being responsible for the rotation of the dipoles Al-V_{Ti}-Al in the lattice of the Ti_3Al phase [34]. In the present paper we focus our attention on the possible influence of Nb on this relaxation peak, which has been measured in the three TNB alloys indicated in Table 1. A series of IF measurement as a function of temperature at different frequencies was performed for each alloy and the corresponding results are plotted in Fig. 2. In all three alloys, a relaxation peak at about 1070 K for 1 Hz is clearly observed, superimposed to a HTB, which is growing very fast on the high temperature side of the IF spectra. It was demonstrated that this HTB is related to the creep behavior [20,33], however this is not the subject of the present work. The IF peak shift towards low temperature when decreasing the frequency and a dynamic modulus variation occurs associated with the peak, which is thus identified with a relaxation peak. The dynamic modulus variation is illustrated in Fig. 2c for the TNB8-Ex alloy, but it is also observed for the other alloys, although it is not plotted for a better clarity of the diagrams. The height of the relaxation peak varies from one alloy to another because it is dependent on the microstructure and the volume fraction of the phases therein.

Due to the fast growing HTB, the shift in temperature of the peak can thus be influenced. Consequently, a precise determination of the activation energy of the relaxation peak requires the subtraction of the HTB as the first step before to proceed with any further analysis. According to Schoeck et al. [45], the HTB follows an exponential behavior and its subtraction requires the corresponding fitting of the HTB to an exponential function. In practice such procedure is performed through the fitting of $Ln(IF)_{HTB}$ versus 1/T to a straight line; this is a standard procedure and does not deserve further comments.

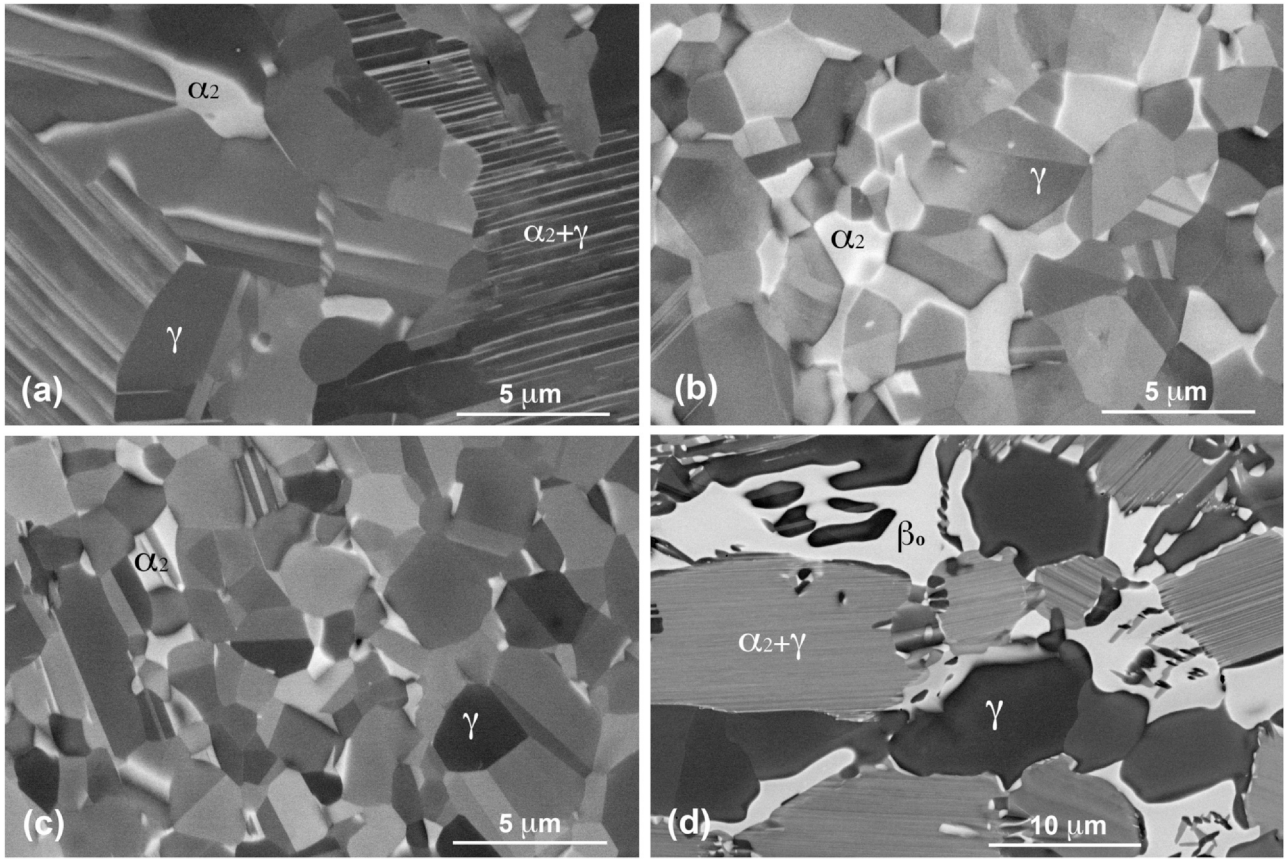

Fig. 1. Scanning electron micrographs taken in backscattered electron mode (10 kV and 0.8 nA) of the three studied alloys: (a) TNB5-PL, (b) TNB-V5 and (c) TNB8-Ex as well as (d) alloy TNM4, which were analyzed by EDX in the same experimental conditions for a better comparison (see Table 1).

Table 1
Nominal composition of the different TiAl alloy variants and Nb concentration in the α_2 phase measured by EDX at 10 kV and 1 nA

Sample	Nominal alloy composition (at%) (balance is Ti)						Nb in α_2 at%	C in α_2 at%
	Al	Nb	Mo	C	Si	B	EDX	APT
TNB8-Ex	45	8	0	0.2	0	0	8.13	0.38
TNB-V5	45	5	0	0.2	0	0.2	5,32	0.38
TNB5-PL	45	5	0	0.2	0	–	5.31	0.38
TNM4	43	4	1	0.02	0	0.1	4.14	0.03
TMS	46.8	0	1	0	0.2	0	0	–

Note: The C concentration in the α2 phase was determined by means of Atom Probe Tomography (APT) and was taken from ref. [20]. The first three alloys are investigated in this study.

Thus, the HTB was subtracted from all the spectra shown in Fig. 2a to c and the corresponding IF peaks are plotted in Fig. 3a to c for the three alloys. It is assumed that the relaxation time of the process follows an Arrhenius behavior, $\tau = \tau_0 \cdot \exp(E_a/k_B T)$. Taking into account that the condition for the IF peak maximum is given for $\omega \cdot \tau = 1$, the activation energy E_a of the process can be easily obtained [23,25] from the expression:

$$Ln(\omega) = -Ln(\tau_0) - \frac{E_a}{k_B \cdot T_P} \quad (1)$$

Plotting the temperature of the maximum of the IF peak, T_P, for each measured frequency in a plot of Ln(ω) versus 1/T a straight line can be fitted, whose slope is E_a/k_B. This procedure was applied to each one of the IF spectra series in Fig. 3a to c, and the corresponding Arrhenius diagrams are displayed for each alloy in Fig. 3d to f, respectively. A straight line is fitted with a correlation factor of R > 0.999 in all cases. The determined activation energies are also indicated in each graph.

It is worthy to note that the samples TNB5-PL and TNB-V5 give exactly the same activation energy, as could be expected because both samples have the same composition, see Table 1, although they come from different producers and exhibit different processing-related microstructures. This fact constitutes a good test on the reproducibility of the IF measurements. Indeed, the activation energy of the relaxation peak P(α_2) as well as its temperature position increases with the Nb content. In Fig. 4a we have plotted the spectra measured at the frequency of 0.1 Hz for the TNB5-PL, the TNB8-Ex and the TNM4 alloy, the last one is taken from the data reported in reference [34]. In addition, we have fitted all experimental peaks to a Debye peak broadened by a Gaussian distribution [23] using the following equation, which gives the mathematical expression of a broadened peak as a function of temperature [25]:

$$Q^{-1} = \tan(\phi) = \tan(\phi)_{max} \cdot \cosh^{-1}\left[\frac{E_a}{r_2(\beta) \cdot k_B} \cdot \left(\frac{1}{T} - \frac{1}{T_P}\right)\right] \quad (2)$$

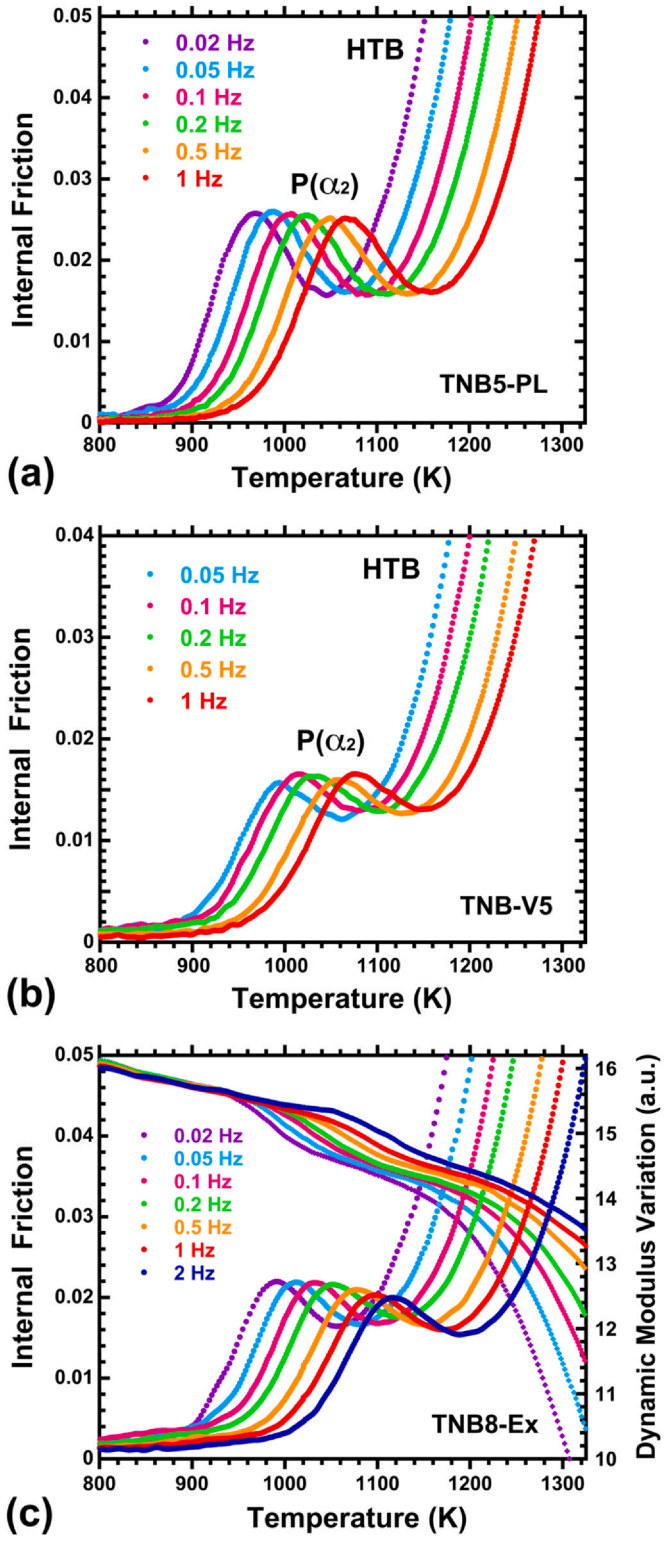

Fig. 2. Experimental internal friction (IF) spectra measured for the three studied alloys at the different indicated frequencies: (a) TNB5-PL, (b) TNB-V5 and (c) TNB8-Ex. The dynamic modulus variation curves, associated with the IF spectra, are also shown in (c).

Here, $r_2(\beta)$ is the broadening factor defined in [23] for a Gaussian distribution, β being the width of the distribution. For a more simple notation, in the following it will be noted that $r_2(\beta) \equiv r$. The best fit for each experimental spectrum is obtained for a different broadening factor r and they are also represented in Fig. 4a. For a better comparison, the best fit of the theoretical spectra, using the corresponding experimental parameters, were normalized and plotted in Fig. 4b. Increasing the Nb content leads to an increased activation energy of the peak P(α_2), which shifts towards higher temperature and, in addition, becomes broader. All these parameters are summarized in Table 2 for comparison.

Nevertheless, the correlation of the activation energy E_a with the Nb content requires a further refinement, because the alloys measured in the present work also contain 0.2 at%C. Recently, it was demonstrated [37] that C atoms also have an influence on the Ti diffusion in the α_2 phase, slightly modifying its activation energy. However, this influence was quantified in [37] and will allow us to estimate the required C-correction. The C solubility is much higher in the α_2 phase than in the γ phase. In fact, the solubility of C in γ at 1000 °C is about 200 ppm [46], whereas it has been estimated to be above 1 at% for the α_2 phase [47–49]. This is because small C atoms preferentially occupy 6Ti-type interstitial octahedral sites in the α_2 phase [46], which are energetically preferred over the 4Ti-2Al octahedral sites in the γ phase [50]. The partition coefficient of C in α_2 and γ phases was precisely determined by atom probe tomography (APT) as described in [17] and, accordingly to the analysis in similar γ-TiAl alloys, e.g. see [20], an average concentration of C = 0.38 at% in the α_2 phase can be estimated from the overall C concentration of 0.2 at% in our alloys. The increment of the activation energy of the peak P(α_2), due to the presence of C, was quantified in $\Delta E = 0.32$ eV × at%C [37], and thus an increase of $\Delta E_a = 0.12$ eV is expected in our alloys when the influence of C atoms is considered. This correction is included in Table 2 and in Fig. 5 the corrected activation energy E_a of the relaxation peak P(α_2) is plotted as a function of the Nb content (at%) present in the α_2 phase. All the alloys included in Table 2 are plotted in Fig. 5, and a straight line fit rather well the dependence of the activation energy E_a on the Nb content, with a slope of $\Delta E_a(\mathrm{Ti}) = 0.037$ eV × at% Nb. This dependence of E_a on the Nb content is much smaller than the dependence of E_a on the C content, but taking into account the respective concentrations used in engineering alloys, the influence of Nb is dominant. Thus, it can be concluded that Nb has a clear effect on the diffusion process responsible for the P(α_2) relaxation, because it increases its activation energy and shifts the peak towards higher temperatures. Understanding the physical origin of these effects requires a deep analysis of the atomic mechanisms responsible for the P(α_2) relaxation process, which will be discussed in the next section.

4. Discussion

The solubility of Nb in α_2-Ti_3Al and γ-TiAl is rather high [8], being distributed in equal amounts in both phases [51], reaching a solubility above 15% in the α_2+γ phase region for the isopleth around 45 at% Al [52]. In fact, Ti and Nb have very similar atomic volumes, that of Nb being slightly bigger, and the Nb atoms occupy substitutional Ti lattice positions in both phases [8]. The diffusion of Nb atoms in Ti_3Al through the exchange with a Ti vacancy V_{Ti} is slower than Ti self-diffusion with an activation energy of $E_a(\mathrm{Nb}) = 3.51$ eV [38] when compared with $E_a(\mathrm{Ti}) = 2.99$ eV [37,53]. In Fig. 6 the lattice of the Ti_3Al phase (Ti in blue and Al in green) is represented with a vacancy V_{Ti} (pink color) in the basal plane and a Nb atom (red color) in the intermediate plane, i.e. at 1/2c axis, although the relative positions of the Nb atom is irrelevant because of the symmetry of the lattice.

The relaxation peak P(α_2) is attributed to the stress-induced rotation of the elastic dipoles Al-V_{Ti}-Al, taking place because of the short distance diffusion of a Ti atom by exchange with a vacancy V_{Ti} in each one of the three equivalent positions [34]. In absence of Nb, the measured activation energy was $E_a(P\alpha_2) = 2.99$ eV [35], corresponding to the Ti self-diffusion in α_2-Ti_3Al [37,53]. Nevertheless, when a vacancy exists at next-neighbor position of a Nb atom, a binding energy $E_B(V_{Ti}\text{-Nb})$ appears, modifying the mobility of the

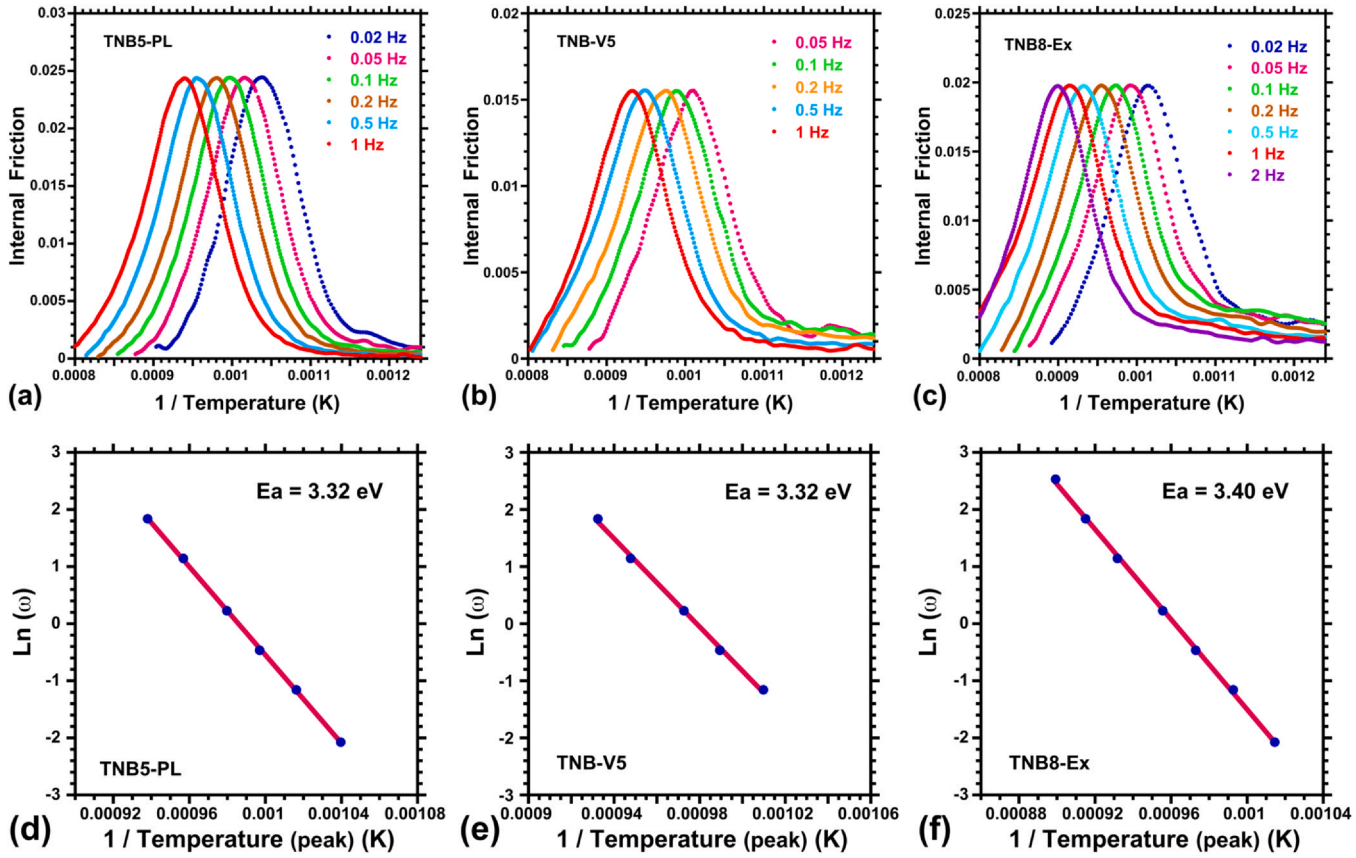

Fig. 3. Internal friction spectra after subtraction of the high temperature background (from Fig. 2) for the three studied alloys: (a) TNB5-PL, (b) TNB-V5 and (c) TNB8-Ex. The corresponding Arrhenius diagrams obtained from the maximum of the peaks are presented in (d), (e) and (f), respectively, and the determined activation energies are indicated.

vacancy. Consequently, the short distance atomic diffusion mechanism responsible for the peak P(α_2) must be also affected by the presence of the Nb atom. In Fig. 7a to c, the atomic configuration of the basal plane in the α_2 phase is depicted, including the projection of the Nb atom (red) in the three possible positions with respect to the vacancy (pink) as well as the three different orientations of the dipole Al-V_{Ti}-Al. Below these schematic images, in Fig. 7d to f, the motion of the vacancy V_{Ti} in the neighborhood of each Nb position is indicated, grouped by pairs (a-d), (b-e) and (c-f), in which the rotation of the dipole is shown for each configuration Nb-V_{Ti}. Here we have to remark that when the condition of a Nb atom at a next neighbor position of the vacancy V_{Ti} is imposed, some dipole configurations are forbidden. For instance the Nb-2 position is not compatible with the dipole configuration shown in Fig. 2a or f. Such dipole configurations are still available for the other Nb-1 and Nb-3 positions. Hence, Fig. 7 shows the six compatible configurations between the Nb atom and the Al-V_{Ti}-Al dipoles. This means, that independently of the Nb position, the stress-induced rotation of the dipole can be still activated, and, consequently, the relaxation process of the peak P(α_2) will occur in a similar way. However, the motion of the Ti atom, exchanging with the vacancy at next-neighbor position of the Nb atom, as shown in each pair of Fig. 7(a–d), (b–e) and (c–f) will require a higher activation energy and, thus, an increase of the activation energy ΔE_a for the peak P(α_2) would be expected, as observed in Fig. 5. Indeed, as the Nb atom is bigger than the Ti atom, it will produce a noticeable expansive lattice distortion and, besides other possible reasons, it can be expected that this makes the motion of a Ti atom at a next neighbor position of the Nb atom more difficult and, therefore, a higher activation energy is required to overcome the saddle point. According to Boltzmann statistics, the activation energy of the relaxation process will be an average of the individual jumps of Ti atoms, with and without the Nb atom at next-neighbor position. The point, however, is that the activation energy of these two local atomic configurations are rather close to each other as to be separated in individual relaxation peaks [23], leading to a continuous distribution of the relaxation times. Hence, in alloys with intermediate Nb content in the α_2 phase, only one apparent peak, including the continuous distribution of both configurations, will be observed. Consequently, the measured activation energy will depend on the relative relaxation strength of each configuration. Thus, the activation energy of the peak P(α_2) will be dependent on the Nb content, as presented in Fig. 5. This increase of the activation energy will be responsible for the shift of the peak towards higher temperatures, as shown in Fig. 4, in agreement with the expectation from a Wert-Marx plot [54]. Obviously, both atomic configurations can also be modified by the presence of interstitial C atoms, which exhibit a similar binding energy E_{BC}(V_{Ti}-C) as reported recently [37]. This is the reason why we have estimated and corrected the influence of C atoms in order to quantify the exclusive influence of Nb on the activation energy of the peak P(α_2).

Another aspect that deserves a comment is the increase of the broadening factor *r* and, consequently, the width of the Gaussian distribution β with the increasing content of Nb, which was presented in Fig. 4. Until now, we have considered that the binding energy E_B(V_{Ti}-Nb) and the local configuration Ti-V_{Ti}-Nb are not dependent on the Nb concentration. However, it should be considered that for high Nb contents, as, for instance, 8 at% in sample TNB8-Ex, the α_2 phase will exhibit one Nb atom for every two cells of the lattice in average. Then, statistically the probability of having Nb atoms at near-next-neighbor positions of other Nb atoms or, what is most important, at near-next-neighbor positions of the vacancy V_{Ti}

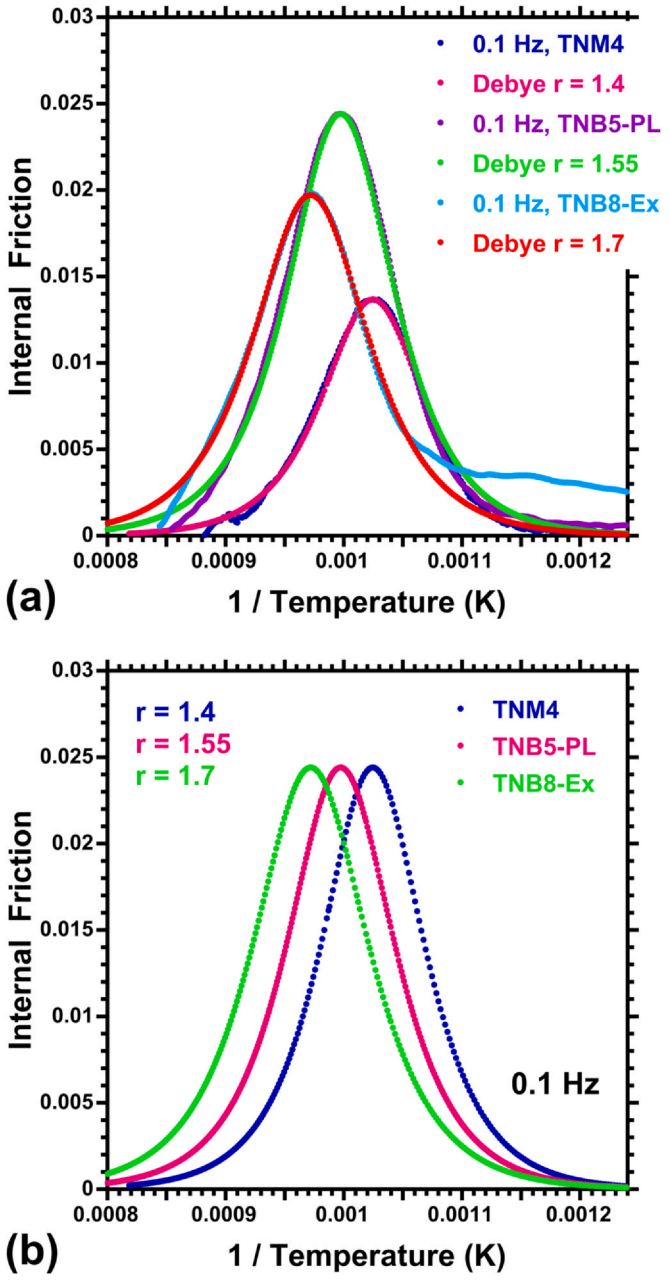

Fig. 4. (a) For comparison, the IF spectra of the samples TNB5-PL and TNB8-Ex are plotted for the same frequency of 0.1 Hz, together with the one of TNM4 from ref. [34]. The fittings of the theoretical broadened Debye peaks, with the indicated broadening parameter, are shown superimposed to the experimental results; (b) the fitted peaks for the three alloys are plotted normalized, allowing a clear comparison of temperature shift as well as broadening.

with a Nb atom at a next-neighbor position, becomes higher with increasing Nb content. This effect will generate a supplementary broadening of the E_a distribution for the Ti-V_{Ti} exchange in such complex local configurations, thus explaining the results of Fig. 4.

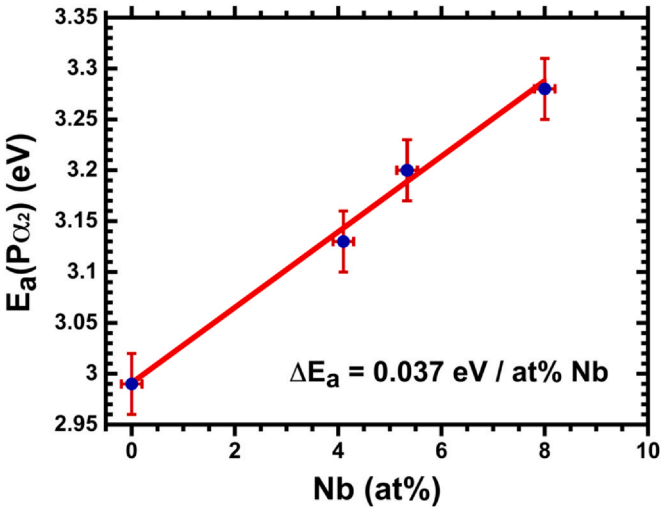

Fig. 5. Dependence of the P(α_2) activation energy on the Nb content. The increment of the activation energy per at% Nb is indicated.

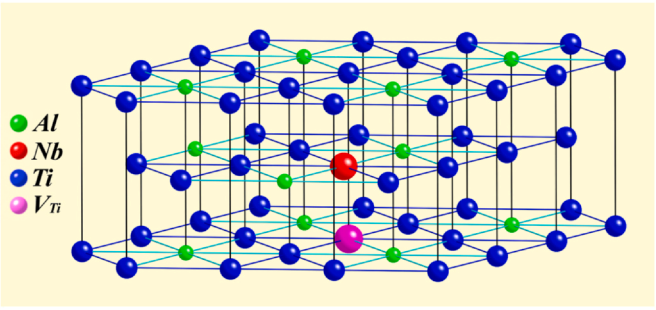

Fig. 6. Atomic lattice of the α_2-Ti_3Al phase (with Ti atoms in blue and Al atoms in green), showing a Ti vacancy V_{Ti} (in pink color) and a substitutional Nb atom (in red color), which have been introduced at a next-neighbor position.

It can be concluded that the proposed atomic model for the internal friction peak P(α_2) allows to explain all experimental observations, in particular the increase of both the activation energy and the broadening factor with increasing Nb content as presented in Figs. 4 and 5.

However, one can be tempted of invoking another scenario in which the peak P(α_2) might be formed from the superposition of two similar, but clearly different mechanisms. The first mechanism would be associated with the jump of a Ti atom by exchange with a vacancy with an activation energy of E_a(Ti) = 2.99 eV, as described above. The second one would be due to the same process, but involving the jump of a Nb atom by exchange with a vacancy, which, according to the diffusion coefficient measured in α_2-Ti_3Al [38], must have an activation energy of E_a(Nb) = 3.51 eV. Nevertheless, in this case the activation of these two processes will generate two independent internal friction peaks with the corresponding activation energy for the short distance diffusion of both atomic species, Ti and Nb. A simple simulation shows that, due to the difference of energies, in this case a clear evidence of the presence of two separated peaks, or at least one peak with a noticeable shoulder at its high-temperature side, should be

Table 2
Broadening factor *r* and Gaussian factor β; measured and C-corrected activation energies of the peak P(α_2) as well as the Nb concentration of the α_2-Ti_3Al phase, see text.

Sample	Broadening factor *r*	Gaussian factor β	Measured E_a P (α_2) (eV)	C-corrected E_a P (α_2) (eV)	Nb at% in α_2 phase
TNB8-Ex	1.7	1.95	3.40	3.28	8.13
TNB-V5	1.6	1.7	3.32	3.20	5.32
TNB5-PL	1.55	1.6	3.32	3.20	5.31
TNM4	1.4	1.3	3.14[34]	3.13	4.14
TMS	–	–	2.99[35]	2.99	0

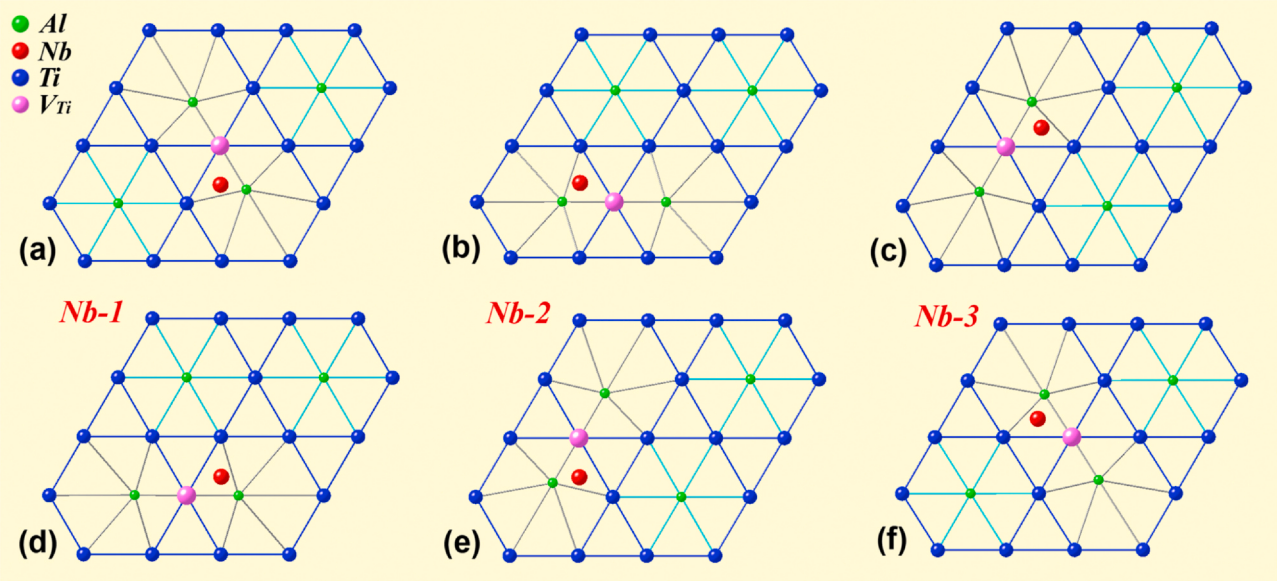

Fig. 7. Schematic view of the basal plane of the α_2 Ti_3Al lattice, where the projections (from 1/2c axis) of the three different sites of the Nb atom (in red color) are indicated in (a), (b) and (c). The sites of the V_{Ti} (in pink color) at next-neighbor position are also indicated, showing the three different possible orientations of the Al-V_{Ti}-Al dipoles. The exchanges Ti-V_{Ti} and the stress-induced rotation of the Al-V_{Ti}-Al dipoles for each one of the three kinds of Nb sites, *Nb-1*, *Nb-2* and *Nb-3* are illustrated in each pair of figures (a-d), (b-e) and (c-f), respectively.

observed. However, the experimental results displayed in Figs. 2 and 3 do not show such evidence and neither do the corresponding fittings (Fig. 4) in any of the measured samples. So, it can be definitely concluded that this explanation is not supported by the experimental results and thus can be discarded.

5. Conclusions

Three intermetallic γ-TiAl based alloys with different Nb contents have been studied by mechanical spectroscopy in order to elucidate the influence of Nb on the relaxation processes at high temperatures. The results have been compared with those from literature obtained for other γ-TiAl based alloys which are leaner in Nb or even Nb-free. The following conclusions can be drawn:

- Mechanical spectroscopy is a powerful tool to characterize the short distance diffusion of point defects through the associated relaxation processes.
- An internal friction peak P(α_2) at about 1070 K for 1 Hz appears in all measured γ-TiAl based alloys, being associated with a relaxation process taking place in the α_2-Ti_3Al phase, which is attributed to the stress-induced rotation of Al-V_{Ti}-Al dipoles, occurring during short distance Ti diffusion by Ti-V_{Ti} exchange.
- The activation energy E_a of the P(α_2) relaxation peak is dependent on the Nb content and the analysis of the obtained results allowed to quantify this dependence as $\Delta E_a(Ti) = 0.037$ eV × at% Nb.
- The peak P(α_2) shift towards higher temperatures and its broadening factor *r* increases with the increasing Nb content.
- An atomic model is proposed, illustrating how the short distance diffusion of Ti and the rotation of the Al-V_{Ti}-Al dipoles are influenced by the next-neighbor V_{Ti}-Nb interaction, giving place to a contribution to the activation energy.
- The proposed relaxation mechanism allows explaining all the observed experimental results, in particular the dependence of E_a on the Nb content as well as the shift in temperature of the peak P(α_2) and its broadening with increasing Nb content.

These findings offer new insights on the impact of Nb, which represents one of the most important alloying elements used for intermetallic γ-TiAl based alloys. The obtained results are very useful for the further design of new advanced γ-TiAl based alloys showing improved high-temperature capabilities.

Declaration of Competing Interest

The authors declare that they have no known competing financial interests or personal relationships that could have appeared to influence the work reported in this paper.

Acknowledgments

The authors thank the financial support from the MINECO, Spain, project CONSOLIDER-INGENIO 2010 CSD2009–00013, as well as by the Consolidated Research Group GIU-17/071 from the University of the Basque Country, UPV/EHU, Spain, and the project ETORTEK CEMAP from the Industry Department of Basque Government, Spain. This work made use of the facilities of the SGIKER from the UPV/EHU, Spain.

References

[1] Y.W. Kim, R. Wagner, M. Yamaguchi (Eds.), Gamma Titanium Aluminides, TMS, Warrendale, 1995.
[2] D.P. Pope, C.T. Liu, S.H. Whang, M. Yamaguchi (Eds.), 4th Conference on High-Temperature Intermetallics, special issue of Mat. Sci. Eng. A 239–240 (1997) 1–928.
[3] Y.W. Kim, D.M. Dimiduk, M.H. Loretto (Eds.), Gamma Titanium Aluminides, TMS, Warrendale, 1999.
[4] Y.W. Kim, H. Clemens, A.H. Rosenberger (Eds.), Gamma Titanium Aluminides, TMS, Warrendale, 2003.
[5] H. Clemens, H. Kestler, Processing and applications of intermetallic γ-TiAl-based alloys, Adv. Eng. Mater. 2 (2000) 551–570.
[6] M. Burtscher, T. Klein, J. Lindemann, O. Lehmann, H. Fellmann, V. Güther, H. Clemens, S. Mayer, An advanced TiAl alloy for high-performance racing applications, Materials 13 (2020) 4720.
[7] F. Appel, R. Wagner, Microstructure and deformation of two-phase γ-Titanium Aluminides, Mater. Sci. Eng. R. 22 (1998) 187–268.
[8] F. Appel, J.D.H. Paul, M. Oehring, Gamma Titanium Aluminide Alloys, Wiley-VCH,, Weinheim, Germany, 2011.
[9] F. Appel, M. Oehring, R. Wagner, Novel design concepts for gamma-base titanium aluminide alloys, Intermetallics 8 (2000) 1283–1312.
[10] F. Appel, U. Brossmann, U. Christoph, S. Eggert, P. Janschek, U. Lorenz, J. Müllauer, M. Oehring, J.D.H. Paul, Recent progress on the development of gamma titanium aluminide alloys, Adv. Eng. Mater. 2 (2000) 699–720.

[11] H. Clemens, W. Wallgram, S. Kremmer, V. Güther, A. Otto, A. Bartels, Design of novel β-solidifying TiAl alloys with adjustable β/B2-phase fraction and excellent hot-workability, Adv. Eng. Mater. 10 (2008) 707–713.
[12] H. Clemens, S. Mayer, Design, processing, microstructure, properties, and applications of advanced intermetallic TiAl alloys, Adv. Eng. Mater. 15 (2013) 191–215.
[13] S. Mayer, P. Erdely, F.D. Fischer, D. Holec, M. Kastenhuber, T. Klein, H. Clemens, Intermetallic β-solidifying γ-TiAl based alloys – from fundamental research to application, Adv. Eng. Mater. 19 (2017) 1–27.
[14] B.P. Bewlay, M. Weimer, T. Kelly, A. Suzuki, P.R. Subramanian, The Science, Technology, and Implementation of TiAl alloys in Commercial Aircraft Engines, MRS Fall Meeting, Boston, USA, 2012.
[15] B.P. Bewlay, S. Nag, M.J. Weimer, TiAl alloys in commercial aircraft engines, Mater. High. Temp. 33 (2016) 549–559.
[16] U. Habel, F. Heutling, C. Kunze, W. Smarsly, G. Das, H. Clemens, Forged intermetallic γ-TiAl based alloy low pressure turbine blade in the geared turbofan, in: V. Venkatesh, A.L. Pilchak, J.E. Allison, S. Ankem, R. Boyer, J. Christodoulou, H.L. Fraser (Eds.), Proceedings of the 13th World Conference on Titanium, John Wiley & Sons Inc, Hoboken, NJ, USA, 2016, pp. 1223–1227.
[17] T. Klein, M. Schachermayer, F. Mendez-Martin, T. Schöberl, B. Rashkova, H. Clemens, S. Mayer, Carbon distribution in multi-phase γ-TiAl based alloys and its influence on mechanical properties and phase transformation, Acta Mater. 94 (2015) 205–213.
[18] M. Kastenhuber, B. Rashkova, H. Clemens, S. Mayer, Enhancement of creep properties and microstructural stability of intermetallic β-solidifying γ-TiAl based alloys, Intermetallics 63 (2015) 19–26.
[19] T. Klein, B. Rashkova, D. Holec, H. Clemens, S. Mayer, Silicon distribution and silicide precipitation during annealing in an advanced multi-phase γ-TiAl based alloy, Acta Mater. 110 (2016) 236–245.
[20] T. Klein, L. Usategui, B. Rashkova, M.L. Nó, J. San Juan, H. Clemens, S. Mayer, Mechanical behavior and related microstructural aspects of a nano-lamellar TiAl alloy at elevated temperatures, Acta Mater. 128 (2017) 440–450.
[21] Z.W. Huang, J.P. Lin, Z.X. Zhao, H.L. Sun, Fatigue response of a grain refined TiAl alloy Ti-44Al-5Nb-1W–1B with varied surface quality and thermal exposure history, Intermetallics 85 (2017) 1–14.
[22] A. Couret, J.-P. Moncoux, D. Caillard, On the high creep strength of the W containing IRIS-TiAl alloy at 850 °C, Acta Mater. 181 (2019) 331–341.
[23] A.S. Nowick, B.S. Berry, Anelastic Relaxation in Crystalline Solids, Academic Press,, New York, 1972.
[24] G. Fantozzi, Introduction to mechanical spectroscopy: Phenomenology and definitions, Mater. Sci. Forum 366-368 (2001) 1–31.
[25] J. San, Juan, Mechanical spectroscopy, Mater. Sci. Forum 366-368 (2001) 32–73.
[26] M.S. Blanter, I.S. Golovin, H. Neuhäuser, H.R. Sinning, Internal Friction in Metallic Materials, Springer-Verlag,, Berlin, 2007.
[27] M. Hirscher, D. Schaible, H. Kronmüller, Internal friction measurements of γ-TiAl, Intermetallics 7 (1999) 347–350.
[28] U. Brossmann, M. Hirscher, H. Kronmüller, Internal friction in γ-TiAl at high temperatures, Acta Mater. 47 (1999) 2401–2408.
[29] M. Weller, A. Chatterjee, G. Haneczok, H. Clemens, Internal friction of γ-TiAl alloys at high temperature, J. Alloy. Comp. 310 (2000) 134–138.
[30] M. Pérez-Bravo, M.L. Nó, I. Madariaga, K. Ostolaza, J. San Juan, High temperature internal friction of Nb-containing γ-TiAl alloys, in: Y.W. Kim, H. Clemens, A.H. Rosenberg (Eds.), Gamma Titanium Aluminides 2003, TMS, 2003, pp. 451–457.
[31] M. Weller, G. Haneczok, H. Kesler, H. Clemens, Internal friction of γ-TiAl-based alloys with different microstructures, Mater. Sci. Eng. A 370 (2004) 234–239.
[32] M. Pérez-Bravo, M.L. Nó, I. Madariaga, K. Ostolaza, J. San Juan, High-temperature internal friction on TiAl intermetallics, Mater. Sci. Eng. A 370 (2004) 240–245.
[33] P. Simas, T. Schmoelzer, M.L. Nó, H. Clemens, J. San Juan, Mechanical spectroscopy in advanced TiAl-Nb-Mo allloys at high temperature, Mater. Res. Soc. Symp. Proc. 1315 (2011) 139–144.
[34] J. San Juan, P. Simas, T. Schmoelzer, H. Clemens, S. Mayer, M.L. Nó, Atomic relaxation processes in an intermetallic Ti-43Al-4Nb-1Mo-0.1B alloy studied by mechanical spectroscopy, Acta Mater. 65 (2014) 338–350.
[35] M. Castillo-Rodríguez, M.L. Nó, J.A. Jiménez, O.A. Ruano, J. San Juan, High temperature internal friction in a Ti-46Al-1Mo-0.2Si intermetallic, comparison with creep behaviour, Acta Mater. 103 (2016) 46–56.
[36] L. Usategui, M.L. Nó, S. Mayer, H. Clemens, J. San Juan, Internal friction and atomic relaxation processes in an intermetallic Mo-rich Ti-44Al-7Mo ($\gamma+\beta_o$) model alloy, Mater. Sci. Eng. A 700 (2017) 495–502.
[37] L. Usategui, T. Klein, M.L. Nó, S. Mayer, H. Clemens, J. San Juan, High-temperature phenomena in advanced intermetallic nano-lamellar γ-TiAl alloy. Part I: Internal friction and atomic relaxation processes, Acta Mater. 200 (2020) 442–454.
[38] J. Breuer, T. Wilger, M. Friesel, C. Herzig, Interstitial and substitutional diffusion of metallic solutes in Ti_3Al, Intermetallics 7 (1999) 381–388.
[39] Y. Mishin, C. Herzig, Diffusion in the Ti-Al system, Acta Mater. 48 (2000) 589–623.
[40] F. Appel, M. Oehring, γ-Titanium aluminide alloys: alloy design and properties, in: C. Leyens, M. Peters (Eds.), Titanium and Titanium Alloys, Wiley-VCH, Weinheim, 2003, pp. 89–152.
[41] V. Güther, M. Allen, J. Klose, H. Clemens, Metallurgical processing of titanium aluminides on industrial scale, Intermetallics 103 (2018) 12–22.
[42] J.A. Jiménez, M. Carsí, G. Frommeyer, S. Knippscher, J. Wittig, O.A. Ruano, The effect of microstructure on the creep behavior of the Ti-16Al-1Mo-0.2Si alloy, Intermetallics 13 (2005) 1021–1031.
[43] I. Gutierrez-Urrutia, M.L. Nó, E. Carreño-Morelli, B. Guisolan, R. Schaller, J. San Juan, High performance very low frequency forced pendulum, Mater. Sci. Eng. A 370 (2004) 435–439.
[44] P. Simas, J. San Juan, R. Schaller, M.L. Nó, High-temperature mechanical spectrometer for internal friction measurements, Key Eng. Mat. 423 (2010) 89–95.
[45] G. Schoeck, J. Shyne, E. Bisogni, Activation energy of high temperature internal friction, Acta Met. 12 (1964) 1466–1468.
[46] A. Menand, A. Huguet, A. Nérac-Partaix, Interstitial solubility in γ and α_2 phases of TiAl-based alloys, Acta Mater. 44 (1996) 4731–4737.
47]] E. Schwaighofer, B. Rashkova, H. Clemens, A. Stark, S. Mayer, Effect of carbon addition on solidification behavior, phase evolution and creep properties of an intermetallic β-stabilized γ-TiAl alloy, Intermetallics 46 (2014) 173–184.
[48] C. Scheu, E. Stergar, M. Schober, L. Cha, H. Clemens, A. Bartels, F.P. Schimansky, A. Cerezo, High carbon solubility in a γ-TiAl-based Ti-45Al-%Nb-0.5C alloy and its effect on hardening, Acta Mater. 57 (2009) 1504–1511.
[49] H. Gabrisch, A. Stark, F.P. Schimansky, L. Wang, N. Schell, U. Lorenz, F. Pyczak, Investigation of carbides in Ti-45Al-5Nb-xC alloys ($0\le x\le 1$) by transmission electron microscopy and high energy-XRD, Intermetallics 33 (2013) 44–53.
[50] D. Holec, R.K. Reddy, T. Klein, H. Clemens, Preferential site occupancy of alloying elements in TiAl-based phases, J. Appl. Phys. 119 (2016) 205104.
[51] R. Kainuma, Y. Fujita, H. Mitsui, I. Ohnuma, K. Ishida, Phase equilibria among α (hcp), β (bcc) and γ ($L1_0$) phases in Ti-Al base ternary alloys, Intermetallics 8 (2000) 855–867.
[52] V.T. Witusiewicz, A.A. Bondar, U. Hecht, T.Y. Velikanova, The Al-B-Nb-Ti system IV. Experimental study and thermodynamic re-evaluation of the binay Al-Nb and ternary Al-Nb-Ti systems, J. Alloy. Compd. 472 (2009) 133–161.
[53] J. Rüsing, Chr Herzig, Concentration and temperaure dependence of titanium self-diffusion and interdiffusion in the intermetallic phase Ti_3Al, Intermetallics 4 (1996) 647–657.
[54] C. Wert, J. Marx, A new method for determining the heat of activation for relaxation processes, Acta Met. 1 (1953) 113–115.